

NUMERICAL SIMULATIONS OF MATHER, FILIPPOV AND CONCENTRIC  
PLASMA FOCUS USING LEE MODEL

FAIRUZ DIYANA BINTI ISMAIL

A thesis submitted in fulfilment of the  
requirement for the award of the degree of  
Doctor of Philosophy (Physics)

Faculty of Science  
Universiti Teknologi Malaysia

JANUARY 2017

I dedicate this thesis to my parents. The most beautiful thing in this world is to see your parents smiling and knowing that you are the reason behind that smile. I love you Ibu and Ayah.

To my husband Mohammad Faiz; the best love is the kind that awakens the soul. That makes us reach for more, that plants the fire in our hearts and bring peace to our minds. That's what I hope to give your forever.

To my son Mohammad Fitri; I've tried and failed at many times in life but I will never stop giving 100% of being the best mom I can be.

Everything they said about how lonely Ph.D journey can be is very true. But I'm very thankful to my family for their endless support throughout good times and hard times.

## ACKNOWLEDGEMENT

Alhamdulillah. Thanks to Allah whom with His willing giving me the opportunity to complete my Ph.D thesis. There are a number of people whom this thesis might not have been written, and to whom I am greatly indebted.

My deepest thanks to Prof. Dr. Jalil Ali who had guided me through this journey. I am mostly grateful to Emeritus Prof. Dr. Lee Sing for his guidance, comment and suggestions. His plasma focus and Lee's code training in the course of my Ph.D research has tremendously accelerated my research progress. I would also like to thank Prof. Dr. Soh Heor Saw for her inputs.

I would like to thanks Universiti Teknologi Malaysia for my study leave opportunity, Ministry of Higher Education (MOHE) for SLAI scholarship funding as well as staff of Laser Centre, Ibnu Sina Institute for Scientific and Industrial Research (ISIS-IR) who have provided the assistance on various occasions and research facilities.

For my fellow labmates; Dr. Kashif, Dr. Natashah, Dr. Ong Shu Teik, Dr. Saiful Najmee, Dr. Nina Diana, Dr. Someira and Dr. Safwan for their much help. Lastly, I truly appreciate the help from Dr. Zuhaib in proof-reading and giving useful physics insights.

## ABSTRACT

In this study, numerical simulations of concentric, Mather and Filippov dense plasma focus (DPF) devices using Lee Model have been performed to test the universality of Lee Model. It includes the configuring of the Lee Model Code to work as any DPF devices from measured current waveform to modelling for diagnostics, evolution of the diagnostics-time histories for the dynamics, energies and plasma properties computed from the measured total current waveform by the code. DPF is a potential source of neutrons. The current research focus is on computing the neutron yield,  $Y_n$ , from DPF by numerical experiments. Published experimental results from these DPF are then compared and analyzed with numerical simulations results in terms of  $Y_n$  at different operational parameters. The numerical simulations were executed using the 5-phase Lee Model Code version RADPFV5.15de. The computed  $Y_n$  from a concentric deuterium-tritium KPU-200 DPF is  $1.44 \times 10^{13}$  neutrons per shot at pressure 14.25 Torr and charging voltage 47.7 kV. For the 1.4 kJ DPF, the optimum,  $Y_n$  was  $2.9 \times 10^7$  neutrons/shot at 5.5 Torr deuterium pressure. The optimum computed  $Y_n$  for 11.2 kJ DPF at 4.1 Torr was  $1.447 \times 10^8$  neutrons/shot. For 28.8 kJ device, the optimum computed  $Y_n$  of  $1.24 \times 10^9$  neutrons/shot was obtained at 2.2 Torr deuterium pressure at 20 kV. For the 480 kJ device, the optimum yield of  $1.8 \times 10^{11}$  neutrons/shot was obtained at pressure 7.6 Torr and charging voltage of 27 kV. Analysis of the results shows that the optimum  $Y_n$  was achieved only at optimum operating conditions. For the Dena Filippov DPF with discharge energies of 5 kJ and 90 kJ at pressures ranging from 0.1 Torr to 2.5 Torr, the computed  $Y_n$  is  $1.5 \times 10^9$  neutrons/shot in agreement with the experimental result of  $1.2 \times 10^9$  neutrons/shot using deuterium gas. The computed  $Y_n$  of Iranian First Filippov Type Plasma Focus (IFFT-PF) with deuterium as working gas at pressure of 0.6 Torr is  $3.4 \times 10^6$  neutrons/shot as compared to the published value of  $3.1 \times 10^6$  neutrons/shot. These results show that the computed  $Y_n$  is in good agreement with the measured  $Y_n$  at charging voltage of 16 kV for Dena device and 26 kV for IFFT-PF. The modelling, results and applications of the Lee Model code are of profound interest.

## ABSTRAK

Dalam kajian ini, simulasi berangka bagi peranti fokus plasma tumpat (DPF) jenis bulatan sepusat, Mather dan Filippov menggunakan Model Lee telah dijalankan untuk menguji keuniversalan Model Lee. Ini termasuk mengkonfigurasi Kod Model Lee supaya boleh diguna untuk semua jenis peranti DPF daripada bentuk gelombang arus terukur kepada permodelan untuk diagnostik, evolusi sejarah diagnostik-masa untuk dinamik, tenaga dan sifat plasma yang dikira daripada jumlah gelombang arus terukur oleh kod. DPF ialah satu sumber berpotensi untuk neutron. Fokus kajian terkini adalah untuk mengira hasil neutron,  $Y_n$ , daripada DPF menggunakan eksperimen berangka. Keputusan eksperimen yang diterbitkan daripada DPF dibanding dan dianalisis dengan keputusan simulasi berangka dari segi  $Y_n$  pada parameter operasi yang berbeza. Eksperimen berangka dilaksana menggunakan Kod Model Lee 5-Fasa, versi RADPFV5.15de.  $Y_n$  yang dikira daripada DPF bulatan sepusat deuterium-tritium KPU-200 ialah  $1.44 \times 10^{13}$  neutron/tembakan pada tekanan 14.25 Torr dan voltan pengecasan 47.7 kV. Untuk peranti 1.4 kJ,  $Y_n$  optimum ialah  $2.9 \times 10^7$  neutron/tembakan pada tekanan deuterium 5.5 Torr.  $Y_n$  optimum yang dikira ialah  $1.447 \times 10^8$  neutron/tembakan untuk peranti DPF 11.2 kJ pada tekanan 4.1 Torr. Untuk peranti 28.8 kJ,  $Y_n$  optimum yang dikira ialah  $1.24 \times 10^9$  neutron/tembakan diperoleh pada tekanan deuterium 2.2 Torr dan voltan pengecasan 20 kV. Bagi peranti 480 kJ, hasil optimum  $Y_n$   $1.8 \times 10^{11}$  neutron/tembakan diperoleh pada tekanan 7.6 Torr dan voltan pengecasan 27 kV. Analisis keputusan menunjukkan  $Y_n$  optimum dicapai hanya pada syarat operasi yang optimum. Bagi peranti DPF Filippov Dena dengan tenaga nyahcas 5 kJ dan 90 kJ pada julat tekanan 0.1 Torr hingga 2.5 Torr,  $Y_n$  yang dihitung  $1.5 \times 10^9$  neutron/tembakan bersetuju dengan hasil eksperimen  $1.2 \times 10^9$  neutron/tembakan menggunakan gas deuterium.  $Y_n$  yang dihitung daripada peranti Iranian First Filippov Type Plasma Focus (IFFT-PF) dengan deuterium sebagai gas bekerja pada tekanan 0.6 Torr ialah  $3.4 \times 10^6$  neutron/tembakan berbanding nilai yang diterbitkan  $3.1 \times 10^6$  neutron/tembakan. Keputusan ini menunjukkan  $Y_n$  yang dihitung bersetuju dengan  $Y_n$  yang diukur pada voltan pengecasan 16 kV untuk peranti Dena dan 26 kV untuk peranti IFFT-PF. Pemodelan, keputusan dan aplikasi kod Model Lee mempunyai kepentingan yang mendalam.

## TABLE OF CONTENTS

CHAPTER	TITLE	PAGE
	<b>DECLARATION</b>	ii
	<b>DEDICATION</b>	iii
	<b>ACKNOWLEDGMENT</b>	iv
	<b>ABSTRACT</b>	v
	<b>ABSTRAK</b>	vi
	<b>TABLE OF CONTENTS</b>	vii
	<b>LIST OF TABLES</b>	xii
	<b>LIST OF FIGURES</b>	xiv
	<b>LIST OF ABBREVIATIONS</b>	xviii
	<b>LIST OF SYMBOLS</b>	xix
<b>1</b>	<b>INTRODUCTION</b>	<b>1</b>
	1.1 Overview	1
	1.2 Physics of Fusion	4
	1.3 Bringing Z-Pinch into Focus	11
	1.4 The Genesis of Plasma Focus Z-Pinch Device	13
	1.4.1 Properties of DPF	15
	1.4.1.1 Energy Density Constancy	16
	1.4.1.2 Scaling Properties of the Plasma Focus	17
	1.5 Problem Statement	19
	1.6 Objectives of the Research	21
	1.7 Scope of the Research	22
	1.8 Significance of the Research	24

1.9	Thesis Outline	27
<b>2</b>	<b>LITERATURE REVIEW</b>	<b>29</b>
2.1	Plasma Focus Device	29
2.2	Neutron Yield Studies of Plasma Focus Device	33
2.3	Neutron Yield Numerical Studies	44
<b>3</b>	<b>THEORY OF PLASMA FOCUS Z-PINCH DEVICE</b>	<b>47</b>
3.1	Introduction	49
3.2	Dynamics of Plasma Focus Devices	50
3.2.1	Operation of Plasma Focus Devices	50
3.2.2	Spherical Plasma Focus	52
3.2.3	Rundown Phase I	54
3.2.4	Rundown Phase II	55
3.2.5	Reflected Shock Phase	56
3.3	The Five Phases of the Lee Model	56
3.4	Axial Phase	58
3.5	Radial Inward Shock Phase	59
3.6	Radial Reflected Shock Phase	60
3.7	Slow Compression (Quiescent or Pinch Phase)	60
3.8	Expanded Column Phase	60
3.9	Governing Equations in Lee's Code Computation	61
3.9.1	Axial Acceleration Phase Description	66
3.9.2	Step-by-step Numerical Integration Functions	70
3.9.3	Radial Phase Description	71
3.9.4	Radial Shock Implosion Phase	73
3.9.5	Radial Shock Reflecting Phase	82
3.9.6	Pinch Phase	85
3.9.6(a)	Plasma Self Absorption	87
3.9.6(b)	Neutron Yield Computation	89
3.9.7	Column Expanding Phase	91

<b>4</b>	<b>RESEARCH METHODOLOGY</b>	<b>93</b>
4.1	Introduction	95
4.2	Philosophy of Lee Modelling	96
4.3	Digitizing of Experimental Data	97
4.4	Radiative Plasma Focus Model (RADPF)	107
4.5	Configuring Spherical Plasma Focus Device with Radiative Plasma Focus Model	109
4.6	Radiation Yield Optimization Process	111
<b>5</b>	<b>RESULTS AND DATA ANALYSIS</b>	<b>114</b>
5.1	Introduction	114
5.2	Fitting the computed current trace to obtain model parameters for spherical plasma focus device	115
5.3	Deuterium-Tritium Filled Spherical Plasma Focus	121
5.4	Deuterium Filled Spherical Plasma Focus	127
5.5	Numerical Experiments on Mather type Plasma Focus	128
5.5.1	Neutron Yield of 1.4 kJ Plasma Focus Device	128
5.5.2	Neutron Yield of IR-MPF-1 Plasma Focus Device	133
5.5.3	Neutron Yield of IR-MPF-100 Plasma Focus	138
5.5.4	Neutron Yield of PF-1000 Plasma Focus Device	142
5.5.5	Relationship between Neutron Yield and Dynamics of Plasma Focus Devices	147
5.6	Numerical Experiments on Filippov type Plasma Focus	154
5.6.1	Numerical Experiments on Dena Plasma Focus Devices operating with Argon	160
5.6.2	Numerical Experiments on Plasma Focus	



	Devices Filippov (IFFT-PF type)	167
5.7	Neutron Yield for Both Devices Mather and Filippov	174
<b>6</b>	<b>CONCLUSION</b>	<b>178</b>
6.1	Future Directions and Conclusions	182
	<b>REFERENCES</b>	<b>183</b>

## LIST OF TABLES

Table No.	Title	Page
2.1	Experimental measured neutron yield from plasma focus devices under different operating parameters	43
3.1	The Governing Equations of Lee Model code	63
5.1	Configured published parameters after successful current fitting for KPU-200 where $L_0$ is the static inductance, $C_0$ is the storage capacitance, $b$ the tube outer radius (cathode), $a$ the inner radius (anode), $z_0$ the anode length, $V_0$ the operating voltage and $P_0$ the operating initial pressure.	118
5.2	Tabulated information from Lee code configured for KPU-200 at 14.25 Torr deuterium-tritium	120
5.3	KPU-200 computed $Y_n$ as a function of pressure, together with some computed pinch properties. $I_{peak}$ is the peak value of the total current, $I_{pinch}$ the plasma pinch current at start of pinch, $T_{pinch}$ the pinch temperature, $v_a$ the axial speed, $v_s, v_p$ the radial shock and piston speeds, $r_{min}$ the minimum radius of focus, $z_{max}$ the maximum length of pinch column, 'pinch dur' the pinch duration, $V_{max}$ the maximum induced voltage and $n_i$ the ion number density	128
5.4	Computed properties of neutron yield optimization for 1.4 kJ plasma focus device	135
5.5	Computed properties of neutron yield optimization for IR-MPF-1 plasma focus device.	141
5.6	Computed properties of neutron yield optimization for PF-	

	1000 plasma focus device	151
5.7	Computed properties of neutron yield optimization for PF-1000 plasma focus device	154
5.8	Relationship between the pressure and drive factor of plasma focus devices.	157
5.9	Neutron-optimized parameters of 1.4 kJ PF, IR-MPF-1, IR-MPF-100 and PF-1000 plasma focus devices with the ratios combining of the $f_m$ , $f_c$ , $f_{mr}$ and $f_{cr}$ values	159
5.10	Published parameters of the plasma focus devices Filippov type	161
5.11	Parameters for Dena device	166
5.12	Computed properties of neutron yield for Dena plasma focus device using deuterium.	169
5.13	Configuration Parameters used for Numerical Experiments with IFFT-PF machine.	173
5.14	Results of neutron emission with different gas pressure in the IFFT- PF	174
5.15	Computed properties of neutron yield optimization for IFFT-PF plasma focus device using $D_2$	175
5.16	Extracted parameters for GN1 Plasma focus into Lee's model code	180

## LIST OF FIGURES

<b>Figure No.</b>	<b>Title</b>	<b>Page</b>
1.1	The D-T fusion reaction at the heart of laser energy	5
1.2	Neutron capture and tritium generation in lithium	6
1.3	Comparison and heating of the fuel capsule, ignition and burn of the D-T fuel	6
1.4	Potential energy schematic for fusion	8
1.5	Principle of Plasma Focus	13
1.6	Schematic of Plasma Focus Z-Pinch device	14
2.1	Three PF devices with different electrodes configurations: (a) Filippov, (b) Mather and (c) concentric	20
3.1	Schematic of plasma sheath dynamics in Mather-type plasma focus device.	50
3.2	Scheme of a plasma focus device shows an approximate cross section in a Filippov type	51
3.3	(a) Concentric plasma focus configuration. (b) Equivalent circuit model of the SPF	52
3.4	Rundown Phase I in concentric PF.	54
3.5	Rundown Phase II in concentric PF.	55
3.6	Reflected Shock Phase in concentric PF.	56
3.7	Five-phase of Lee model	57
3.8	Equivalent circuit diagram of plasma focus device.	62
3.9	The relationship between magnetic piston and shock front where $r_p$ , $r_s$ and $v_p$ , $v_s$ are the instantaneous position and the speed of the magnetic piston and shock front respectively. (a) is the side view plasma	

	slug motion and (b) shows the cylindrical shape of plasma slug	72
3.10	The schematic diagram of start of radial reflected shock phase when shock front at $r_s = 0$ .	83
3.11	Cross sections for D-T, D-D(total) and D-He3 reaction	91
3.12	Schematic diagram of beam-target neutron yield mechanism.	92
4.1	A schematic flow diagram on the philosophy of Lee Modelling	97
4.2	GetData Digitizer working platform and selecting an image to start-off digitizing data.	99
4.3	Set Xmin value	100
4.4	Set Xmax value	101
4.5	Adjust the scale for Xmin, Xmax, Ymin and Ymax	102
4.6	Choose the area to digitize by holding the mouse button and drag the mouse to cover all area.	103
4.7	Screenshots of post-digitizing the discharge current	104
4.8	With an eraser tool, erase the unnecessary points	105
4.9	Save the workspace	106
4.10	Export the digitize data to XLS (Microsoft Excel) format	107
4.11	Simplified flow chart for step by step GetData Graph Digitizer	108
4.12	RADPF V5.15de xls working platform	110
4.13	Example of digitized data compilation into the Lee Code version RADPF 5.15de and the experimental measured current profile plotted from the digitized data.	112
4.14	Flow chart of radiation yield optimization process	114
4.15	Flow chart of radiation yield optimization process	115
5.1	Published measured current waveform for KPU-200 for deuterium-tritium mixture at pressure 14.25 Torr	117
5.2	Measured current waveform compared with computed	119

	current waveform for KPU-200 at 14.25 Torr deuterium-tritium gas at 25 kV	
5.3	PNK-13 plasma neutron chamber design	121
5.4	(a) Calculated and measured discharge current compared with (b) computed and measured current fitting performed with Lee code.	122
5.5	(a) Neutron yield versus pressure (b) further increase the pressure until 50 Torr.	124
5.6	Computed current waveform as a function of pressure. The basis of reference is a measured waveform at 14.25 Torr which is used to fit the computed 14.25 Torr waveform to obtain the model parameters.	125
5.7	Neutron Yield as a function of voltage DT	127
5.8	(a) Neutron Yield as a function of Pressure, (b) Neutron Yield as a function of Voltage DD	131
5.9	Computed and measured current profile fitting for 1.4 kJ plasma focus operated at 4.5 Torr (D <sub>2</sub> ) and 10 kV	132
5.10	Positions of shock front and magnetic piston for 1.4 kJ plasma focus device.	133
5.11	Computed and measured current profile fitting for IR- MPF-1 plasma focus operated at 3.2 Torr (D <sub>2</sub> ) and 40 kV	138
5.12	Positions of shock front and magnetic piston for IR- MPF-1 plasma focus device.	139
5.13	Computed and measured current profile fitting for IR- MPF-100 plasma focus operated at 1.9 Torr (D <sub>2</sub> ) and 20 kV	144
5.14	Positions of shock front and magnetic piston for IR- MPF-100 plasma focus device.	145
5.15	Computed and measured current profile fitting for PF- 1000 plasma focus operated at 3.5 Torr (D <sub>2</sub> ) and 27 kV	148
5.16	Positions of shock front and magnetic piston for PF- 1000 plasma focus device.	152

5.17	(a) Pinch duration comparison between 1.4 kJ and IR-MPF-1 (11.2 kJ) plasma focus devices, and (b) pinch duration comparison between IR-MPF-100 (29 kJ) and PF-1000 (480 kJ) plasma focus devices.	155
5.18	The different output of Lee Model modified Lee Model Code shown in (a), (b), (c).	165
5.19	A typical current signal fitted to measured signal at $P=0.45$ Torr and charging voltage 16 kV	167
5.20	Computed neutron yield ( $Y_n$ ) versus pressure ( $P$ ) using deuterium	170
5.21	Pinch time ( $t_p$ ) as a function of pressure.	171
5.22	Positions of shock front and magnetic piston for Dena device	172
5.23	The computed neutron yield with measured neutron yield in the IFFT-PF	176
5.24	Current signal fitted to measured signal at $P=0.65$ Torr and charging voltage 31kV for IFFT device	177
5.25	Positions of shock front and magnetic piston for IFFT-PF	178
5.26	Pinch duration comparison between Dena and IFFT-PF plasma focus devices	179
5.27	Measured current waveform compared with Lee's model computed current waveform for GN1 at 3 Torr deuterium gas from published data.	181
5.28	The neutron yield for both devices Mather and Filippov	182

**LIST OF ABBREVIATIONS**

PF	-	Plasma Focus
RADPF	-	Radiative Dense Plasma Focus
UNU-ICTP	-	United Nations University/International Centre for Theoretical Physics
PMT	-	Photomultiplier Tube
BIC	-	Baise Ion Collector
MCNPX	-	Monte Carlo Simulation Package
KSU	-	Kansas State University
HV	-	High Voltage
SXR	-	Soft X-ray
CCD	-	Charge Coupled Device
SDS	-	Small Disturbance Speed
JPEG	-	Joint Photographic Experts Group
xls	-	Microsoft Excel 2007 binary file



## LIST OF SYMBOLS

$L_o$	-	Static Inductance
$L$	-	Plasma Inductance
$L_a$	-	Axial Phase Inductance
$C_o$	-	Capacitance
$V_o$	-	Charging Voltage
$r_o$	-	Stray Resistance
$b$	-	Radius of Circle Formed by Cathode Rods Surrounding the Central Anode
$a$	-	Anode Radius
$z$	-	Instantaneous Position
$z_o$	-	Anode Length
$P_o$	-	Gas Pressure
$f_m$	-	Axial Phase Mass Sweeping Factor
$f_{mr}$	-	Radial Phase Mass Sweeping Factor
$f_c$	-	Axial Phase Current Factor
$f_{cr}$	-	Radial Phase Current Factor
$Y_n$	-	Neutron Yield
$Y_{th}$	-	Thermonuclear Neutron Yield
$Y_{b-t}$	-	beam-target Neutron Yield
$V_p^{max}$	-	Maximum Voltage Drop During The Pinch
$\Delta E_p^{max}$	-	Maximum Energy Transfer To The Pinch
$\Delta I$	-	Change In Discharge Current Trace
$I$	-	Circuit current
$I_o$	-	Characteristic Current
$I_{pinch}$	-	Pinch Current
$I_{peak}$	-	Peak Current
$E_o$	-	Device's Energy

RESF	-	Ratio Of Stray Resistance To Impedance
EINP	-	Work Done By The Radial Magnetic Piston
Si	-	Silicon
H	-	Hydrogen
H <sup>2</sup> or H <sup>3</sup>	-	Hydrogen Isotopes
He	-	Helium
Cu	-	Copper
Al	-	Aluminum
Ti	-	Titanium
Ar	-	Argon
Ne	-	Neon
D <sub>2</sub>	-	Deuterium Gas
H <sub>2</sub>	-	Hydrogen gas
Be	-	Beryllium
$Y_{sxr}$	-	Soft X-ray Yield
$c$	-	$b/a$
$\vec{j}$	-	Current Density
$\vec{B}$	-	Magnetic Field
$p$	-	Momentum
$m$	-	Object's mass
$r_s$	-	Shock Front Position
$r_p$	-	Magnetic Piston Position
$z_f$	-	Pinch Length
$v$	-	Velocity
$v_a$	-	Characteristic Axial Current Sheath Speed
$v_s$	-	Radial Shock Front Speed
$v_p$	-	Radial Magnetic Piston Speed
$v_r$	-	Characteristic Radial Inward Shock Speed
$\rho_o$	-	Ambient Density
$F$	-	Magnetic Force
$\mu$	-	Permeability
$R$ or $r$	-	Plasma Resistance
$\tau$	-	Time In Normalized Form

$\zeta$	-	Current Sheath Axial Position in Normalized Form
$I$	-	Current In Normalized Form
$Z_o$	-	Surge Impedance
$t$	-	Time
$t_o$	-	Characteristic Discharge Time
$t_a$	-	Characteristic Current Sheath Travelling Time In Axial Phase
$t_r$	-	Characteristic Current Sheath Travelling Time In Radial Phase
$D$	-	Incremental Time
$P_m$	-	Magnetic Pressure
$P$	-	Shock Pressure
$\gamma$	-	Specific Heat Ratio
$Z_{eff}$	-	Effective Charge Number
$dV$	-	Pinch Slug Volume
$\kappa_s$	-	Shock Front Position In Normalized Form
$\kappa_p$	-	Magnetic Piston Position In Normalized Form
$\zeta_f$	-	Pinch Length In Normalized Form
$\Delta t$	-	Time Lapse Between The Shock Front And Magnetic Piston
$D_c$	-	Departure Coefficient
$k_B$	-	Boltzmann's constant
$m_p$	-	Proton Mass
$R_o$	-	Universal Gas Constant In SI Units
$T$	-	Shock Plasma Temperature
$Q_J$	-	Joule Heating Energy
$Q_B$	-	Bremsstrahlung Energy
$Q_{rec}$	-	Recombination Energy
$Q_L$	-	Line Radiation Energy
$N_i$	-	Ion Number Density
$N_o$	-	Ambient Number Density
$Z_n$	-	gas atomic number
$A$	-	self-absorption corrected factor

$M$	-	photonics excitation number
$V_{\max}$	-	induced voltage
$T_{pinch}$	-	Pinch Temperature
$r_{min}$	-	Minimum Pinch Radius
$z_{max}$	-	Maximum Pinch Length
Xmin	-	Minimum Value of X-axis
Xmax	-	Maximum Value of X-axis
Ymin	-	Minimum Value of Y-axis
Ymax	-	Maximum Value of Y-axis
$t_{p-dur}$	-	Pinch Duration

## **CHAPTER 1**

### **INTRODUCTION**

#### **1.1 Overview**

The scientific discoveries of the early 1900's, led by Einstein, enabled Man to control the processes within the atom leading to electronics, lasers, computers, global communications, aerospace transportation, new materials, nanotechnology, biotechnology and nuclear energy. Thus continues the era of human prosperity on a greater scale than ever before with corresponding increase in energy consumption and population increase.

World population grew from the 450 million in 1500 to 1.6 billion around 1900 to 6.8 billion towards end 2009. In the past 100 years world population grew 4 times, whilst energy consumption grew 10 times. Thus energy consumption grew faster than population, in other words energy consumption per head also grew more than 2 times. This trend of energy consumption growth is bound to continue as the rest of the world marches relentlessly to catch up with the standard of living of the United States of America. Significantly as is well-known, per capita consumption of energy is closely correlated with standard of living.

In the past 100 years the doubling time of world population was about 50 years whilst the doubling time of energy consumption was 30 years. If this trend were to continue, world population would reach 27 billion in another hundred years

whilst energy consumption would increase another 10 times. This is of course unsustainable as the world is already near the critical point when supply of energy barely meets the demand. Energy resources are limited and supply trends are estimated to peak in a few short decades from now. This is the reason underlying demographers' projections that world population growth must slow down in the near future.

As our understanding of the environmental impact of fossil fuel based energy production increases, it is becoming clear that the world needs a new energy solution to meet the challenges of the future. A transformation is required in the energy market to meet the need for low carbon, sustainable, affordable generation matched with security of supply. In the short term, an increasing contribution from renewable sources may provide a solution in some locations. In the longer term, low carbon, sustainable solutions must be developed to meet base load energy demand, if the world is to avoid an ever increasing energy gap and the attendant political instabilities. The current debate on the unsustainability of population growth, energy consumption trends and the degradation of the environment, whilst important in raising public awareness, does not address the fundamental problem.

What is needed to safeguard Mankind's unimpeded progress is not incremental moves; but one giant bold step - the development of a new limitless source of energy, clean non-polluting energy which will not further aggravate the environment.

Nuclear fusion energy may offer such a solution. Fusion energy has the potential to make a substantial contribution to meeting world energy needs in the second half of this century.

There are numerous benefits of fusion energy. In terms of security of supply and sustainability fusion provides energy security and avoids geopolitical constraints because the key components of the fuel, deuterium and lithium, are abundant and widely distributed. There are sufficient materials available for global power production at the 1TWe (terawatt electrical) level for more than 1000 years.

Fusion energy is intrinsically very safe since it carries no risk of thermal runaway. There is little stored energy within the system, no critical mass issues and, under fault conditions, energy production would simply stop.

The environmental impact is low. There are no carbon emissions from the fusion energy production process. With the use of suitable materials for the reaction vessel, the relatively small amount of radioactive waste generated from neutron activation will be short lived with the appropriate choice materials are already available.

Fusion energy is an affordable energy. Financial modeling based on reasonable assumptions of progress during the next phase of technology development and ignition physics shows that electricity derived from laser fusion may well be cost competitive with other environmentally acceptable sources[2], although the energy landscape in 30–50 years is uncertain and hence difficult to predict.

In the last ten years the pace of development for fusion as an energy source has noticeably quickened. Energy and climate sustainability have moved to centre stage. As a consequence, the fusion community is starting to look forward collectively to the day that fusion energy becomes a commercial reality. The principle of thermonuclear fusion is simple but its realization for commercial energy production is technologically extremely demanding.

The technology is already nearly proven. Fifty years of scientific and technological work have already shown that the technology is feasible. Moreover the last final push is set to begin with an international consortium comprising the major economic and scientific communities of the world. The project is ITER-the International Thermonuclear Experimental Reactor which is currently being built in France at Cadarache. The process involves nuclear fusion which is the same process occurring in the stars causing their glow and powering all the energetics of the universe, including all life on earth. Nature is thus showing the way, powering the whole universe with nuclear fusion. Man is in the process of emulating nature.

In 30-50 years time, with human control of this limitless clean non-polluting energy, Man's scientific and technological progress can continue to accelerate, human population can continue to grow. With limitless energy, materials can be created or mined in extra-terrestrial territories like our Moon or further afield from the planets. Living space can be extended by extra-terrestrial colonization which will also serve as energy production bases to avoid overheating the earth. Man's will to explore, up the mountains, down to the sea floors, to the heart of the atom, to the very fabric of space-time; to colonize, as shown in the Americas and Australia, and to grow, should not be stifled by a limit to energy or a limit to population. Man's spirit must, will remain indomitable. As Columbus reached for the Americas in the not too distant past 500 years ago, in the not too distant future, Man will reach for the stars. The best years for fusion physics are still to come.

## 1.2 Physics of Fusion

Two main approaches to fusion, namely inertial and magnetic confinement are under intensive study in the scientific community. Fusion by inertial confinement, in which a minute fuel capsule is highly compressed (to more than one thousand times its liquid density) until ignition occurs in the centre and spreads outwards into the surrounding cold fuel. Ignition lasts as long as the fuel remains confined by its own inertia. A stationary burn is thus impossible with inertial confinement. In this approach,  $n \sim 10^{31} \text{m}^{-3}$  and  $t_E \sim 10^{-11} \text{s}$ ;  $t_E$  is the time during which the fuel freely expands [3].

In inertial fusion the reaction confinement is essentially at the sound speed or thermal disassembly time ( $3 \times 10^{-11} \text{s}$  at  $T = 1 \text{ keV}$ ). Laser-driven IFE as shown in Fig. 1.1 is based on the conversion of isotopes of hydrogen into helium through the process of fusion, using lasers as a driver. This technology could be producing energy on the 2050 timescale, with the potential to supply significant proportion of world energy needs in the following decades. IFE has progressed from an elusive



phenomenon of physics to a predictable, controllable technological process, ready to be harnessed for the benefit of mankind.

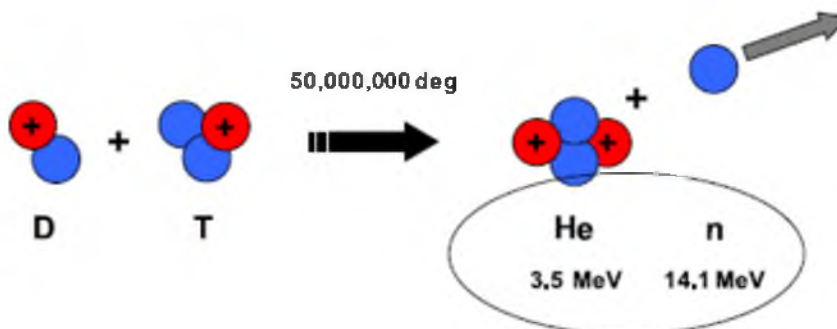


**Figure 1.1,** The D-T fusion reaction at the heart of laser energy [3].

There are several potential fusion reactions, but the deuterium and tritium reaction has the highest cross section under the conditions attainable on Earth and is thus the most favorable for energy production in the foreseeable future chemical means. Tritium, however, is radioactive with a half-life of 12.3 years and must be generated 'in situ' within the fusion fuel cycle. The process, which is based on neutron capture by lithium, is illustrated in Figure 1.2. Lithium is abundant and widely distributed in the Earth's crust. It can also be extracted from seawater.

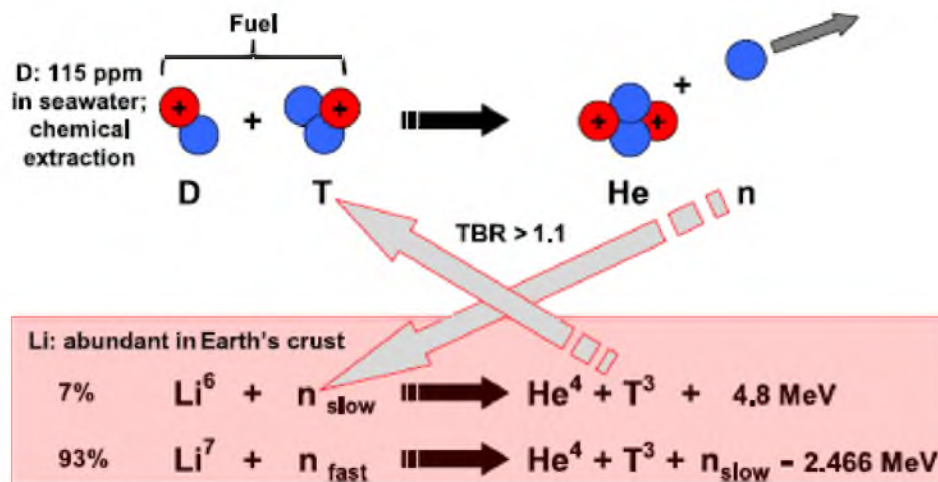


Figure 1.2, Neutron capture and tritium generation in lithium [3].

The process of compression and heating by the laser is shown schematically in Figure 1.3.

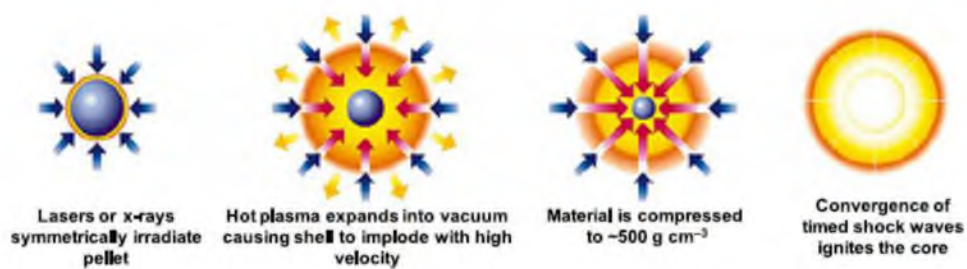


Figure 1.3, Comparison and heating of the fuel capsule, ignition and burn of the D-T fuel [3].

The underlying physics involves the use of powerful lasers to heat a mixture of two hydrogen isotopes, deuterium and tritium, to an extreme temperature of greater than 50 million degrees, whereupon the constituent nuclei fuse to form a helium ion (alpha particle) and a neutron, according to the reaction shown in Figure 1.1. In each fusion reaction, the helium ion and the neutron carry excess energy totaling 17.6 MeV.

In fusion, the products of reaction have less mass than the constituents. The mass loss,  $m$ , is released as energy,  $E$ , according to Einstein's familiar equation  $E=mc^2$ , where  $c$  is the velocity of light. Since the velocity of light is very large, a relatively small mass loss corresponds to a very large energy release.

The physics of fusion is based on the joining of light elements. When light nuclei approach to a separation comparable to their diameter, the strong nuclear force draws them even closer together until they fuse. However, this force only acts over very short distances. At larger separation the nuclei are subjected to the repulsive Coulomb force which acts to push them apart. Only nuclei with sufficient kinetic energy to overcome the Coulomb barrier can approach closely enough to fuse. At room temperature an insignificant number of nuclei possess such energy, and external heating must be applied. It is the requirement to supply this heat energy that gives rise to the term thermonuclear.

The height of the Coulomb barrier for deuterium and tritium is 1 MeV, corresponding to a temperature of 10 billion K. Fortunately, quantum mechanical tunneling enables a significant number of neutrons to penetrate the barrier at lower energy, reducing the heating requirement to 5 keV (50 million K). These two competing forces are shown in Figure 1.4, as a potential energy or 'bowling ball' diagram. The induction of fusion can be considered in terms of rolling a ball up the Coulomb potential with sufficient speed, or temperature, that it reaches the top of the barrier and falls into the potential well created by the strong nuclear force.

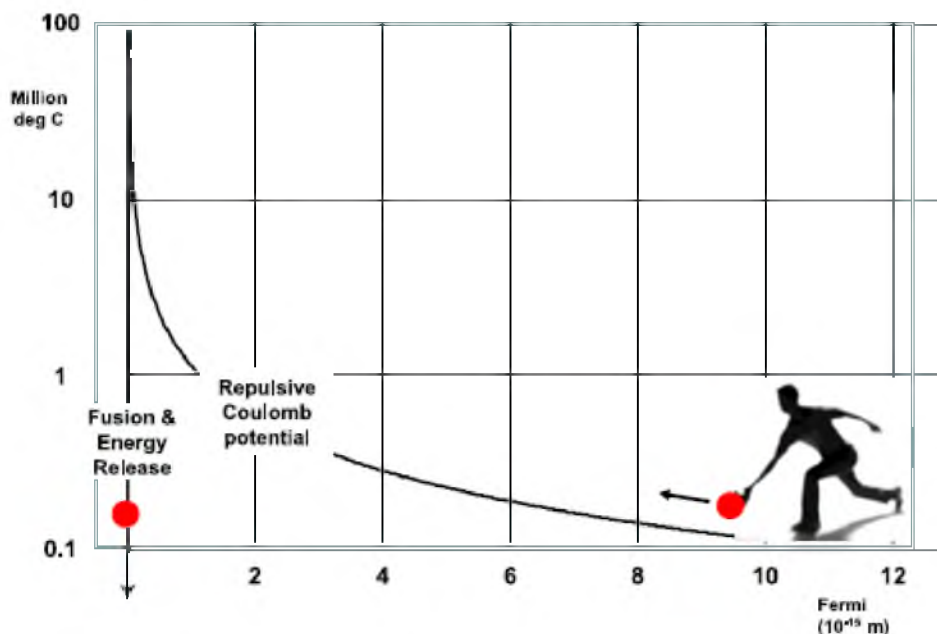


**Figure 1.4,** Potential energy schematic for fusion [3]

The liberated energy from fusion reactions has the same nuclear origins as fission but there is an important difference between the physics of the two reactions which explains why power production from fusion is so technologically demanding. In the case of fission, some high atomic number nuclei are unstable and undergo spontaneous fission to produce lower atomic number products and energetic neutrons. These reactions occur at room temperature without the need to supply external energy to initiate or sustain them.

Einstein's  $E=mc^2$  enabled Man to understand the energy source of the universe. Man's control of  $E=mc^2$  is demonstrated in the awesome power of his Hydrogen bomb. Man will liberate his destiny with  $E=mc^2$  in nuclear fusion reactors. This is the Dawning of the Fusion Age.

Fusion by magnetic confinement, in which hot plasma is confined by magnetic fields forming a magnetic trap for the charged particles. In theory, a stationary burn is possible for as long as the magnetic confinement is maintained. (In this approach,  $n \sim 10^{20} \text{ m}^{-3}$  and  $t_E \sim 1$  to 5 s). In magnetic confinement the plasma is held by magnetic fields in the desired configuration for reaction times large (up to 1

s) compared to its disassembly time at the speed of sound, or the particle thermal speed.

When matter is heated to a high enough temperature, it ionizes and becomes plasma. It emits electromagnetic radiation. The spectrum depends on the temperature and the material. The higher the temperature and the denser the matter, the more intense is the radiation. Beams of electrons and ions may also be emitted. If the material is deuterium, nuclear fusion may take place if the density and temperature are high enough. In that case neutrons are also emitted. Typically the temperatures are above several million K and compressed densities above atmospheric density starting with a gas a hundredth of an atmospheric density.

One way of achieving such highly heated material is by means of an electrical discharge through gases. As the gas is heated, it expands, lowering the density and making it difficult to heat further. Thus it is necessary to compress the gas whilst heating it, in order to achieve sufficiently intense conditions. An electrical discharge between two electrodes produces a constricting magnetic field which pinches the column. In order to pinch, or hold together, a column of gas at about atmospheric density at a temperature of 1 million K, a rather large pressure has to be exerted by the pinching magnetic field. Thus an electric current of at least hundreds of kA are required even for a column of small radius of say 1 mm. Moreover the dynamic process requires that the current rises very rapidly, typically in under  $0.1 \mu\text{s}$  in order to have a sufficiently hot and dense pinch.

One of the earliest and least complicated plasma fusion confinement ideas to be identified is the Z-pinch configuration. Z-pinch and Dense Plasma Focus (DPF) are two promising devices for bringing fusion power. In fact the Z-pinch is the oldest method used in order to generate high-temperature dense magnetized plasmas DMP has been based on high-current pulsed discharges between metal electrodes.

The Z-Pinch and the dense plasma focus device is an magneto-inertial fusion MIF concept in which a column of gas is converted to plasma and then compressed

to thermonuclear conditions by an axial current. MIF is an approach which has been shown to potentially lead to a low cost, small reactor for fusion break even.

A Z-pinch is a deceptively simple plasma configuration in which a longitudinal current produces a magnetic field that tends to confine the plasma. The Z designation refers to the direction of the current in the device referring to the z axis in an x, y, z (three-dimensional) coordinate space. A current runs through two plates. The current ionizes a gas and forms a plasma. In its simplest form, a Z-pinch device uses the axial electric current in a plasma column to generate an azimuthal magnetic field that compresses the plasma, or pinches it down. Magnetic pressure from the azimuthal field confines and compresses the column, creating a hot, dense plasma. The plasma then self-pinches. In a Z-pinch device, a cylinder of plasma collapses on itself, momentarily producing extremely high temperatures, and pressures at the center of the cylinder as well as very high electric fields.

Z-pinches have been a subject of interest since the 1950s, when they were explored as a possible avenue for creating fusion power. The simple geometry and low cost made it an early candidate for controlled fusion experiments. At that time, research with pinch devices in the United Kingdom and U.S. proliferated. However, instabilities in the plasma led to this effort being abandoned. The experiments still created neutron which is a classic signal of fusion. It just wasn't thermonuclear fusion, which is what scientists thought was needed to achieve energy gain. Magnetohydrodynamics instabilities usually destroy the pinch within few nanoseconds thus limiting its usefulness. Some of draw backs of classical Z-pinch device includes the mismatch in between pinching time and maximum of discharge current, contamination of pinch by insulator material and the stability of pinch column.

However, instabilities and rapid plasma loss motivated the development of more complicated plasma confinement systems such as tokamaks and stellarators. Recent experiments, in which z-pinches produced unprecedented levels of radiation and power, have led to renewed interest in the configuration. As a result, z-pinch research is currently one of the fastest growing areas of plasma physics, with revived

interest in z-pinch controlled fusion reactors along with investigations of new z-pinch applications, such as, very high power x-ray sources, high-energy neutrons sources, and ultra-high magnetic fields generators.

Scientists tried to overcome these demerits of classical Z-pinch. Researchers from LANL and Kurachatov Institute came out with a new electrode geometry Z-pinch device that addressed these demerits. Super-fast super-dense pinch that requires special MA fast-rise (ns) pulsed-line were introduced. These lines may be powered by capacitor banks, and suffer the disadvantage of conversion losses and high cost due to the high technology pulse-shaping line, in addition to the capacitor banks.

There is a view that whereas Tokamaks and laser implosions will likely be the devices to succeed in the efforts to harness nuclear fusion, these are huge programmes which will take extraordinary amounts of combined international resources and cooperation on a scale never before attempted. Ongoing research on other devices such as pinches has shown that these are able to produce nuclear fusion even in devices of much smaller scales; even table-top size devices.

### **1.3 Bringing Z-Pinch into Focus**

Nuclear fusion is a key subject which will grow in world-wide importance as ITER project progresses towards maturity. Major break-throughs are indeed coming now with plasma Tokamak ITER (International Thermonuclear Experimental Reactor), laser system NIF (National Ignition Facility) and smaller scale systems such as pinches and the DPF.

DMP are produced in the laboratory by high-current pulsed discharges, e.g. those of the Z-pinch or plasma-focus (PF) type. DMP produced by different devices, such as plasma accelerators, Dense Plasma Focus (DPF), pinch facilities, etc., occupies a niche between the inertial plasma fusion devices (e.g. of the laser-

produced implosion plasma types) and the installations with the magnetic plasma confinement (for example, of the tokamak type). This niche is established by characteristic times of physical processes and by the respective plasma parameters.

The z-pinch discharge is one of the most studied pulsed -power schemes. In a Z-pinch discharge, hot plasmas are created by converting the kinetic energy of an electromagnetically driven imploding sheath into thermal energy. A Z-pinch is a radial implosion of a cylindrical or annular plasma under the influence of a strong magnetic field produced by current flowing down the length of the plasma; it usually involves the ionization and subsequent implosion of a gas for time-scales on the order of microseconds. The process can be broken down into a number of steps that occur in the following order such as gas injection(pre-ionization), compression(implosion), stagnation(burn) and expansion(explosion).

A superior method of producing the super-dense and super-hot pinch is to use the DPF. Not only does this device produce superior densities and temperatures, moreover its method of operation does away with the extra layer of technology required by the expensive and inefficient pulse-shaping line. A simple(though large) capacitor discharge is sufficient to power the DPF.

The plasma focus combines feature of both the EM shock tube and the Z-pinch in such a properly sequenced manner that all the features of both devices may be demonstrated in one single device.

The plasma focus is often regarded as a kind of the dynamic r-pinch because of its radially contracting current channel. Historically, however, it has developed from the coaxial Marshall plasma gun and the Filippov non-cylindrical plasma sheath compression device. Progress in focus research has been achieved rather by experimental skill and brilliant intuition than by theoretical deliberations by, in particular, pioneers like Mather, Bostick and the Filippov couple.

After the declassification of fusion research in the late 1950s, a series of ideas and papers emerged on ways to produce fusion using z-pinches. In 1965, J.W.



Mather and a team at Los Alamos National Laboratory (LANL) published results showing remarkable neutron yields from a relatively compact, low-current generator: a dense plasma focus (DPF). Data did show that this laboratory-scale device was a powerful neutron source but, alas, the neutrons were created by instability mechanisms rather than a bulk thermal process. Work over the next 25 years showed that these DPF devices could scale to about  $1 \times 10^{12}$  neutrons in pure deuterium (D) experiments but that was the limit. Now in 2014, with the two DPF research and development facilities in Nevada, the U.S. Department of Energy (DOE)/National Nuclear Security Administration (NNSA) now has the highest current DPF capability in America and is using it to further several DOE missions. The DPF machines at the Nevada National Security Site (NNSS) are producing intense (up to  $10^{13}$ ) 14.1 MeV neutrons per burst, and short (less than 100 ns) pulses of either 2.45 or 14 MeV neutrons from nuclear fusion using D or DT gases [25, 26].

#### 1.4 The Genesis of Plasma Focus Z-Pinch Device

In a DPF, the physics used allows the slow capacitor discharge (many microseconds) to be converted into a rapid energy compression (less than 100 ns). Inside a dense plasma focus machine, light gases are heated and magnetically compressed to conditions similar to those inside the sun.



**Figure 1.5,** Principle of Plasma Focus

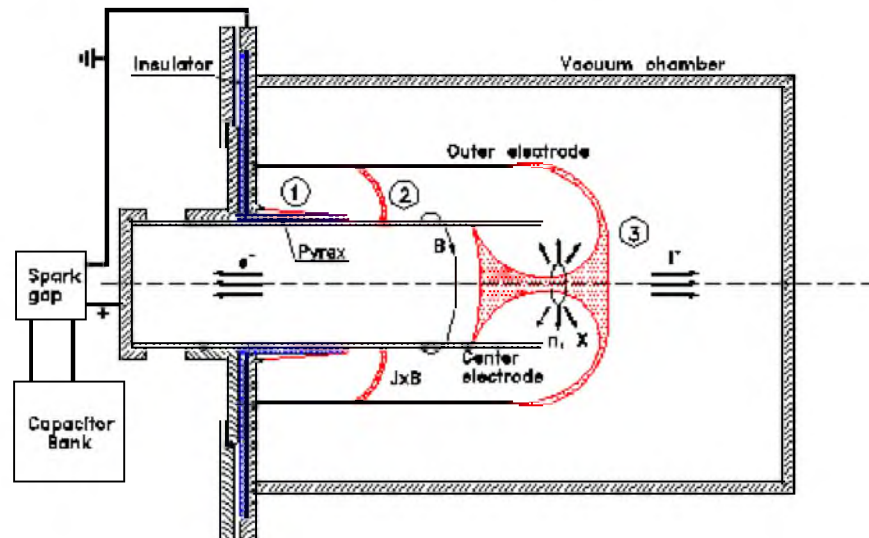


**Figure 1.6,** Schematic of Plasma Focus Z-Pinch device

A DPF Z-pinch consists of two coaxially located electrodes with a high-voltage source connected between them, typically a capacitor bank. When the high-voltage source is energized with a low-pressure gas in the chamber, a plasma sheath forms at one end of the device. In the run down phase, the plasma sheath is pushed down the outside length of the inner electrode, ionizing and sweeping up neutral gas as it accelerates. When the plasma sheath reaches the end of the electrode, it begins to collapse radially inward during the run in phase. In the final pinch phase, the plasma implodes, creating a high-density region that typically emits high-energy electron and ion beams, x rays, and neutrons.

DPF machines use many gases, including deuterium and tritium. The insulating gas becomes ionized, transforming into current-carrying plasma. The plasma is pushed to the reaction point in the tube at the end of the anode, as shown in Figure 1.6. There the intense magnetic fields compress the plasma into a very small volume, making it dense and hot; hence the name dense plasma focus. The final compression process is called a z-pinch. Temperatures and pressures of the plasma reach extreme conditions like those on the outer parts of stars. The DPF is not hot or dense enough to produce fusion like in a star, but plasma instabilities do produce some very local heating and some very energetic beams of deuterons. These cause

neutrons to be emitted. From start-to-finish, the whole process lasts but a few millionths of a second; the fusion processes last for less than a millionth of a second. Neutrons are emitted in a tiny volume about the size and shape of a short piece of pencil lead, a cylinder roughly 1 mm in radius and 10 mm long. Neutrons are emitted at rates up to  $10^{20}$  per second. A coaxial plasma accelerator that produces high-temperature, high-density short lived plasma, temp.  $\sim 1\text{-}4$  keV, density  $\sim 10^{25\text{-}26}\text{m}^{-3}$  Time  $\sim 100\text{-}200$  nsec.

#### 1.4.1 Properties of DPF

The DPF is an interesting fusion device for generating particle beams (ions, electrons and neutrons) and is a very powerful source of ionizing EM radiations starting from visible to X-rays,  $\gamma$ -rays. DPF produces plethora of interesting phenomenon of hot spots, plasmoids, current filamentations, instabilities, turbulences.[26]

It produces nanosecond pulses of:

- Directed powerful hot ( $T \sim 1$  keV) fast ( $v > 10^7$  cm/s) dense ( $n_{pl} \approx 10^{16} \dots 10^{19}$  cm<sup>-3</sup>) plasma streams,
- High-energy ion ( $E_i \approx 0.01 \dots 100$  MeV) and electron ( $E_e \approx 0.01 \dots 1.0$  MeV) beams
- Soft ( $E_{hv} \sim 0.1 \dots 10$  keV) and hard ( $E_{hv} \sim 10 \dots 1000$  keV) X-Rays and
- Fusion neutrons (monochromatic  $E_n \sim 2.45$  and  $14$  MeV as well as broad-range ones,  $2 - 11.3$  MeV)

These streams may irradiate a target with power flux density on its surface equal to  $10^5\text{W}/\text{cm}^2$  (for neutrons),  $10^8\text{W}/\text{cm}^2$  (for soft and hard X-rays),  $10^{10}\text{W}/\text{cm}^2$  (for fast ion streams and plasma jets) and up to  $10^{13}\text{W}/\text{cm}^2$  (for self-focused electron beams).[15,23,26]

Compared with classical accelerators, fission reactors and isotopes a DPF is an ecologically friendlier radiation-producing device because:

- It uses low charging voltage ( $\sim 10$  kV)
- It becomes a radiation source just for a few nanoseconds only on demands (*a push-button source*)
- It is a radiation-safe device, i.e. it has no fission materials and doesn't need any special containers for the device's preservation.

DPF having very short pulse duration of radiation simultaneously with very high energy contained in the pulse can be used in pulsed radiation physics, chemistry and biology.[27,30]

#### 1.4.1.1 Energy Density Constancy

The smallest sub-kJ pF and the large PF have practically [9, 10, 12]:

- The same energy density (per unit mass)
- The same temperature
- The same speeds.
- The dense hot plasma pinch of a small  $E_0$  plasma focus and that of a big  $E_I$  plasma focus have essentially the same energy density, and the same mass density.
- The big  $E_I$  plasma focus has a bigger physical size and a bigger discharge current. The size of the plasma pinch scales proportionately to the current and to the anode radius, as does the duration of the plasma pinch.
- The bigger  $E_I$ , the bigger ' $a$ ', the bigger  $I_{peak}$ , the larger the plasma pinch and the longer the duration of the plasma pinch. The larger size and longer duration of the big  $E_I$  plasma pinch are essentially the properties leading to the bigger neutron yield compared to the yield of the small  $E_0$  plasma focus.
- Voltage and pressure do not have any particular relationship to  $E_0$ .
- Peak current  $I_{peak}$  increases with  $E_0$ .

- Anode radius ' $a$ ' increases with  $E_0$ .
- $ID$  (current per  $cm$  of anode radius)  $I_{peak}/a$  is in a narrow range from 160 to 210  $kA/cm$
- $SF$  (speed or drive factor)  $(I_{peak}/a)/P_0^{0.5}$  is 82 to 100  $kAcm^{-1}/Torr^{0.5}$  deuterium gas
- Peak axial speed  $v_a$  is in the narrow range 9 to 11  $cm/us$ .
- Fusion neutron yield  $Y_n$  ranges from  $10^6$  for the smallest device to  $10^{11}$  for the largest PF.
- It is emphasized that the  $ID$  and  $SF$  are practically constant at around 180  $kA/cm$  and  $(90 kA/cm)/Torr^{0.5}$  deuterium gas throughout the range of small to big devices,  $Y_n$  changes over 5 orders of magnitude.

#### 1.4.1.2 Scaling Properties of the Plasma Focus

A range of plasma focus devices ranging from sub-kJ pF and the large PF in the radial phase. have practically the following properties [16-19].

- The pinch temperature  $T_{pinch}$  is strongly correlated to the square of the radial pinch speed  $v_p$ .
- The radial pinch speed  $v_p$  itself is closely correlated to the value of  $v_a$  and  $c=b/a$ ; so that for a constant  $v_a$ ,  $v_p$  is almost proportional to the value of  $c$ .
- The dimensions and lifetime of the focus pinch scale as the anode radius ' $a$ '.

$r_{min}/a$  (almost constant at 0.14-0.17)

$z_{max}/a$  (almost constant at 1.5)

- Pinch duration has a relatively narrow range of 8-14  $ns$  per  $cm$  of anode radius.
- The pinch duration per unit anode radius is correlated to the inverse of  $T_{pinch}$ .

$T_{pinch}$  itself is a measure of the energy per unit mass. It is quite remarkable that this energy density at the focus pinch varies so little (factor of 5) over a range of device energy of more than 3 orders of magnitude.

This practically constant pinch energy density (per unit mass) is related to the constancy of the axial speed moderated by the effect of the values of  $c$  on the radial speed.

The constancy of  $r_{min}/a$  suggests that the devices also produce the same compression of ambient density to maximum pinch density; with the ratio (maximum pinch density)/ (ambient density) being proportional to  $(a/r_{min})^2$ . So for two devices of different sizes starting with the same ambient fill density, the maximum pinch density would be the same.

From the above discussion, we may put down as rule-of-thumb the following scaling relationships, subject to minor variations caused primarily by the variation in  $c$  in the following:

- Axial phase energy density (per unit mass)                      constant    axial speed
- Radial phase energy density (per unit mass)                      constant    radial speed
- Pinch radius ratio    constant
- Pinch length ratio    constant
- Pinch duration per unit anode radius                                      constant

Today, there is a rich community of laboratories using DPF machines for a wide variety of purposes, ranging from basic plasma physics to applied physics. There has been a recent resurgence in the use of these machines facilitated by much better theoretical tools that are leading to improved understanding of the complex z-pinch process. Large range of phenomena observed in easily constructed PF devices leads to its study in many laboratories.

## 1.5 Problem Statement

While DPFs were invented and optimized over six decades ago, the operative plasma physics processes are yet to be fully understood. The DPF system that produces fusion is simple in concept while also being a product of a rich combination of scientific and engineering disciplines. There is an increasing interest in unconventional approaches to thermonuclear fusion energy from magnetically confined plasmas. The reason is that fusion fuel can be seen as energy and neutron rich.

The dense plasma focus of the wide Filippov type or the slim Mather type is a plasma compression device producing a highly energetic plasma of a small size and a short lifetime [1,2]. Its geometry is hardly compatible with presently envisaged thermonuclear fusion reactor concepts. However, its capability as a remarkably intense fusion neutron source is well-established and recognized for materials testing and, potentially, as the fusion neutron source in a hybrid reactor. The focus plasma neutron yield exceeds that expected from calculations based on data from a thermal plasma by two or more orders of magnitude only when operated with a proper matching of the external power source to the focus electrodes, and if a number of experimental parameters have been identified and adjusted for high neutron yield.

Although many questions regarding the efficient operation of PF devices for fast ion, fast electron, X-ray and neutron emission had been solved, there remains still a lot to be done to properly understand and control processes taking place, especially at the beginning and the end of a discharge. The variation in the proportion of neutrons produced in thermonuclear reactions and beam-target interaction and their scaling with the input energy are still a subject of investigation. This study concentrates on the neutron emission of concentric, Mather and Filipov PF devices.

Plasma focus is one of the smaller scale devices which complement the international effort to build a nuclear fusion reactor. This leads to high neutron yield

output as one of the main goals of plasma focus research. With so many potential technological applications of neutrons from plasma focus devices, during the last five decades, substantial effort and resources have been invested in plasma focus devices. Different plasma focus configurations gives different interesting physics insights. Thus there are many unresolved issues. The Mather and Filippov type plasma focus are well known device on the linear design. Most of the experiments all over the world are performed with the PF cylindrical configurations.

In the past, people were working on z-pinches and linear PFs. Most researcher weren't interested in specifically using the electric fields produced in these devices which are related to neutron generation. These fields were considered a by-product and a nuisance, because most researchers were focused on using the devices for thermonuclear fusion. There were some very early papers on the quasi-concentric configuration of a PF and the neutrons produced. The simplest configuration was a set of two conical, hemiconcentric or plane electrodes placed at a chosen distance inside a vacuum chamber.

Since its invention in 1950s, the DPF has diversified into many configurations, some very different from each other. One technique to better understand the PF implosion and neutron dynamics is to make significant changes to the conventional geometrical PF configuration into concentric PF. However, such devices were not well enough understood to harness the neutrons they produced. This novel concentric PF configuration may have applications to HED science and laboratory astrophysics as well as enhancing and testing the understanding of cylindrical wire array implosions.

Most of the simulation are done using either the MHD, particle in cell or Lee model for Mather type and Filippov type but not the concentric devices. In the numerical aspects, the Lee's code, consists of the combination of snow plow model and slug model, has been used for comprehensive studies on modeling of plasma focus. Our interest is to use Lee model to simulate the concentric PF devices.



The concentric plasma focus is completely different from the conventional linear Filippov-and Mather-type devices. It has a special design where the chamber is in sphere shape. It was first developed in 1996 at the Scientific Research Institute of Experimental Physics, Sarov, Russia. The anode (cylindrical part of anode is covered by an insulator tube) and cathode of the device are in concentric shape and the anode is enclosed by the cathode.

Similarly, the concentric electrode shows the most stable neutron emission with consistently good neutron yield and the relative hard x-ray yield was the highest for hemiconcentric design. The neutron yield is about  $10^{13}$  which is relatively high as compared to other experiments. The charging voltage is high but is still low as compared to other PF experiments. However, either neutron yield or x-ray produced by  $J \times B$  is not clearly identified since current density is produced from the source but magnetic field is produced from plasma. Hence, the essential problem to be resolved in PF research has always been to discover the physics, which dominates the configuration, a question closely related to the neutron production mechanism and plasma dynamics.

## 1.6 Objectives of the Research

The general objective of this research is to investigate Lee modeling of plasma dynamics and neutron yield in concentric plasma focus devices.

The specific objectives of this research are;

- To model the dynamics of current sheath in concentric plasma, Mather and Filipov plasma focus with Lee Model
- To determine, using Lee Model, the neutron yield,  $Y_n$ , for different performance parameters

- To compare the computed neutron yield,  $Y_n$  obtained from concentric, Mather and Filipov PF with the measure yield.

## 1.7 Scope of the Research

In this study, numerical simulations for concentric, Mather and Filipov plasma focus devices using Lee model has been performed. It includes the configuring of the Lee Model Code to work as any PF devices from measured current waveform to modelling for diagnostics, evolution of the diagnostics-time histories for the dynamics, energies and plasma properties computed from the measured total current waveform by the code.

The current research focus is on the computing the neutron yield from the DPFs by numerical experiments. Published experimental results from these plasma focus devices are then compared and analyzed with numerical simulations results in terms of neutron yield at different operational parameters.

The numerical experiments were executed using the 5-phase Lee Model Code, version RADPFV5.15de. The code was configured for the plasma focus devices with energies ranging from 1.4 kJ – 480 kJ using the available published parameters such as inductance,  $L_o$ , capacitance,  $C_o$ , charging voltage,  $V_o$  stray resistance,  $r_o$ , radius of the cathode,  $b$ , anode radius,  $a$ , anode length,  $z_o$ , gas pressure,  $P_o$  and the molecular weight, atomic number of filling gas and the current signal. It is known that the current trace of the focus is one of the best indicators of gross performance of the DPFs. The axial and radial phase dynamics and the crucial energy transfer into the focus pinch are among the important information that is quickly apparent from the current trace. The exact time profile of the total current trace is governed by the bank parameters, by the focus tube geometry and the operational parameters. It also depends on the fraction of mass swept-up and the fraction of sheath current and the variation of these fractions through the axial and radial phases. These parameters determine the axial and radial dynamics, specifically

the axial and radial speeds which in turn affect the profile and magnitudes of the discharge current.

There are many underlying mechanisms in the axial phase such as shock front and current sheet structure, porosity and inclination, boundary layer effects and current shunting and fragmenting which are not simply modeled. Likewise in the radial phase mechanisms such as current sheet curvatures and necking leading to axial acceleration and ejection of mass, and plasma current disruptions. The detailed profile of the discharge current is influenced by these effects and during the pinch phase also reflects the Joule heating and radiative yields. Thus the discharge current powers all dynamic, electrodynamic, thermodynamic and radiation processes in the various phases of the plasma focus. Conversely all the dynamic, electrodynamic, thermodynamic and radiation processes in the various phases of the plasma focus affect the discharge current. The discharge current waveform contains information on all the dynamic, electrodynamic, thermodynamic and radiation processes that occur in the various phases of the plasma focus. This explains the importance attached to matching the computed total current trace to the measured total current trace in the procedure adopted by the Lee model code. Once matched, the fitted model parameters assure that the computation proceeds with all physical mechanisms accounted for, at least in the gross energy and mass balance sense. The current profiles fitting between the computed against experimental were performed. The mass sweeping factors and the current factors for axial and radial phase were used as the fitting coefficient. The model computes the neutron yield, for operation in deuterium, using a phenomenological beam-target mechanism. The model does not compute a time history of the neutron emission, only a yield number  $Y_n$ . In this modeling each factor contributing to the yield is estimated as a proportional quantity and the yield is obtained as an expression with proportionality constant. The yield is then calibrated against a known experimental point. A plot of experimentally measured neutron yield  $Y_n$  vs  $I_{pinch}$  was made combining all available experimental data. Then, optimizations of yields were conducted numerically as a function of pressure. The model code when properly fitted is able to realistically model any plasma focus and act as a guide to diagnostics of plasma dynamics, trajectories, energy distribution and gross plasma properties.

## 1.8 Significance of the Research

Some of the significance of this DPF research can be explored numerically, experimentally or discussed hypothetically, which might be of interest for scientists and engineers working in this field.

Dense plasmas can be produced by means of transient electrical discharges. In particular, a pinch is a transient plasma column conducting electrical current, which becomes self-confined by the associated magnetic field. Plasma pinches reproduce the scenario of high-energy-density, intense beams of charged and neutral particles, with radiation emission. Thus, they become a suitable laboratory tool for fundamental and applied research on fusion and neutron production, among other phenomena.

The most natural use of DPF in science is its application for research in the field of basic plasma physics, fundamental research and education.. With this device, relatively simple and cheap in comparison with the modern nuclear fusion devices like NIF, NX or JET, many phenomena of dense magnetized plasma dynamics, plasma transport properties, turbulence, etc., may be investigated.

DPF is also an excellent device for training students in various disciplines of general physics education. Since it produces high temperature plasma and different types of ionizing radiation it can be used in a modern laboratory for studies of thermodynamics, electromagnetism, atomic physics, optics and spectroscopy, nuclear physics, etc. Special advantage of this apparatus as an equipment for modern physics laboratory in University is that it is ecologically clean in comparison with isotopes. It becomes a radiation source only for a few ns during the discharge through gas.

It can also be used for training in specialized disciplines like plasma physics, plasma diagnostics, nuclear methods, material sciences, etc., for graduating students. Postgraduates and PhDs can explore this facility for fundamental scientific

investigations and industrial applications using many different types of radiation emitted from this pulsed powerful source.

PF involving compact directional neutron sources. Particle accelerators are a fundamental tool of modern science for advancing high-energy and nuclear physics, understanding the workings of stars, and creating new elements. The machines produce high electric fields that accelerate particles for use in applications such as cancer radiotherapy, nondestructive evaluation, industrial processing, and biomedical research. The steeper the change in voltage—that is, the more the voltage varies from one location to another—the more an accelerator can “push” particles to ever-higher energies in a short distance.

The DPF thus holds significant promise for compact neutron sources compared with conventional technology. Mobile sources with peak neutron outputs exceeding  $\sim 10^{15}$  n/s should be feasible with some engineering development.

It provides an avenue to study scaling law for neutron yield as DPF as a very intense neutron source. Scaling laws for the neutron yield formulated at the beginning of the plasma focus investigations were very promising for these devices. Later investigations however, carried out on bigger devices suggested that there is a certain energy limit above which scaling laws saturates.

With current accelerator technologies, electric-field gradients for ion accelerators are limited to approximately 30 megavolts per meter and low peak currents. These studies allow us to better understand the acceleration mechanisms in Z-pinch machines. Scientists may eventually be able to use Z-pinches created from dense plasma foci for compact, scalable particle accelerators and radiation-source applications. With this simple technology, electric-field gradients greater than 100 megavolts per meter and with kiloampere-class peak currents may be possible.

The biggest devices of this type have current on the level of several MA and pulsed magnetic fields of about several megagauss. Self-focusing relativistic electron beams carry the energy up to hundreds kJ and produce at the anode surface a power

flux density of more than  $10^{17}$  W/m<sup>2</sup>. All these features result in corresponding pressures on a megabar level, which is far beyond of the strength of materials. These facts make large DPF devices a tool for investigation of a matter under extreme conditions.[15,23]

The study of plasma focus device has been widely and actively researched for its concept, design, construction, various physics phenomena operation as well as the proper and better improvement of diagnostics techniques for each application purpose. Apart from application purpose, the research is also important to be investigated numerically for development in educational area. Therefore, by incorporating the numerical modification of thermodynamics data based on extensive improvement of plasma ionization balance calculation, more realistic design and product is possibly achieved for better yield and energy resolution in plasma focus study. This study will improvise the calculations in consideration which was yet to be explored. Thus, it contributes to the comprehension of the DPF by providing a demonstration in the numerical experiments and explaining the uncovered aspects of this phenomenon.

Results assembled from the numerical experiments and data collected from actual experimentations are useful to enable in obtaining a greater insight of the physics of the real processes in a plasma focus device. Therefore, the numerical method for improving plasma dynamics in the plasma focus devices that will affect the radiation yields especially for the plasma compression is investigated. This is a highly cost effective method for exploring a lot of complex physical phenomena which are not possible by actual experiments. Working on solving this problem seemingly simple to start with we had deepened our understanding of the plasma focus.

Unlike nuclear reactors that emit neutrons over a broad range of energies, DPF fusion devices are fairly mono-energetic. This characteristic is beneficial for many types of physics experiments, for instance, measuring nuclear cross-sections. Also, the DPF emits neutrons in very short bursts, allowing for fast time resolution. Furthermore, DPF machines are quite compact in comparison to large accelerators

that are used as neutron sources; this makes them ideal for applications where space is at a premium or where transportability is required. These defining characteristics provide a research and application niche in which the DPF excels as a tool to accomplish high quality research quickly and efficiently.

The DPFs can be used for a wide variety of physics experiments, including stockpile stewardship instrumentation development, the measurement of physical quantities such as material properties, nuclear cross-sections, and for quantifying the performance of specialized systems, ranging from homeland security (e.g., radiochemistry activation experiments) to national defense issues (e.g., improvised nuclear devices)[26].

Important new applications such as Neutron Diagnosed Subcritical Experiments (NDSE), which dynamically measure reactivity, are currently being explored. The purpose of this class of experiment is to quantify the neutron multiplication (“chain reaction”) that is the fundamental mechanism that generates energy in nuclear weapons. Neutron multiplication is extremely sensitive to compressibility of materials, and understanding compressibility under the conditions encountered in a nuclear weapon primary will be a key factor in guarding against problematic aging effects, and establishing the safety/security characteristics for the future stockpile. To be successful as one of several candidate pulsed neutron sources for these experiments, the DPF will need to generate a neutron pulse of the desired profile and a width of 50 nanoseconds (at 2 meters flight path), have a trigger jitter less than  $\pm 100$  nanoseconds[26].

## **1.9 Thesis Outline**

Chapter 1 provides a brief introduction on the overall review of the research background, work undertaken including the problem statement, objectives, scope, significance of the study and the research outline. The literature review with particular emphasis on the neutron yield is introduced in Chapter 2. Chapter 3 describes theoretical framework of DPFs in relation to the governing equations

involved in modelling of concentric, Mather and Filippov DPF. Chapter 4 provides a description on the research methodology and the underlying philosophy of the Lee Code modeling. Chapter 5 describe results obtained from simulation of Lee Model with concentric, Mather and Filippov devices over different DPF energies. Chapter 6 concludes the studies.



## REFERENCES

1. Nukulin, V.Y. and Polukhin, S.N., (2007). Saturation of the neutron yield from megajoule plasma focus facilities. *Plasma Physics Reports*, 33(4), pp.271-277.
2. Meehan, T., (2012). Overview of NSTec Plasma Focus Tubes and Magnetohydrodynamic Modeling Capabilities.
3. Edwards, C.B. and Danson, C.N. (2015) 'Inertial confinement fusion and prospects for power production', *High Power Laser Science and Engineering*, 3.
4. Lee, S. A Sequential Plasma-Focus. *IEEE Transactions on Plasma Science*, 1991. 19(5): 912-919.
5. Verma, R., R.S. Rawat, P. Lee, A.T.L. Tan, H. Shariff, G.J. Ying, S.V. Springham, A. Talebitaher, U. Ilyas, and A. Shyam. Neutron Emission Characteristics of NX-3 Plasma Focus Device: Speed Factor as the Guiding Rule for Yield Optimization. *Ieee Transactions on Plasma Science*, 2012. 40(12): 3280-3289.
6. Wong, D., A. Patran, T.L. Tan, R.S. Rawat, and P. Lee. Soft X-ray optimization studies on a dense plasma focus device operated in neon and argon in repetitive mode. *IEEE Transactions on Plasma Science*, 2004. 32(6): 2227-2235.
7. Castillo-Mejia, F., M.M. Milanese, R.L. Moroso, J.O. Pouzo, and M.A. Santiago. Small plasma focus studied as a source of hard X-ray. *Ieee Transactions on Plasma Science*, 2001. 29(6): 921-926.
8. Patran, A., L.C. Tan, D. Stoenescu, M.S. Rafique, R.S. Rawat, S.V. Springham, T.L. Tan, P. Lee, M. Zakaullah, and S. Lee. Spectral study of the electron beam emitted from a 3 kJ plasma focus. *Plasma Sources Science & Technology*, 2005. 14(3): 549-560.
9. Lee, S. and S.H. Saw. Plasma focus ion beam fluence and flux—For various gases. *Physics of Plasmas*, 2013. 20(6).
10. Lee, S. and S.H. Saw. The plasma focus-trending into the future. *International Journal of Energy Research*, 2012. 36(15): 1366-1374.
11. Zakaullah, M., K. Alamgir, M. Shafiq, M. Sharif, and A. Waheed. Scope of plasma focus with argon as a soft X-ray source. *Ieee Transactions on Plasma Science*, 2002. 30(6): 2089-2094.

12. Bures, B.L., M. Krishnan, and R.E. Madden. Relationship Between Neutron Yield and Macroscale Pinch Dynamics of a 1.4-kJ Plasma Focus Over Hundreds of Pulses. *Ieee Transactions on Plasma Science*, 2011. 39(12): 3351-3357.
13. Damideh, V., A.A. Zaeem, A. Heidarnia, A. Sadighzadeh, M.A. Tafreshi, F.A. Davani, M. Moradshahi, M.B. Mahmoudi, and R. Damideh. Design and Fabrication of 11.2 kJ Mather-Type Plasma Focus IR-MPF-1 with High Drive Parameter. *Journal of Fusion Energy*, 2012. 31(1): 47-51.
14. Salehizadeh, A., A. Sadighzadeh, M.S. Movahhed, A.A. Zaeem, A. Heidarnia, R. Sabri, M.B. Mahmoudi, H. Rahimi, S. Rahimi, E. Johari, M. Torabi, and V. Damideh. Preliminary Results of the 115 kJ Dense Plasma Focus Device IR-MPF-100. *Journal of Fusion Energy*, 2013. 32(2): 293-297.
15. Gribkov, V.A., A. Banaszak, B. Bienkowska, A.V. Dubrovsky, I. Ivanova-Stanik, L. Jakubowski, L. Karpinski, R.A. Miklaszewski, M. Paduch, M.J. Sadowski, M. Scholz, A. Szydlowski, and K. Tomaszewski. Plasma dynamics in the PF-1000 device under full-scale energy storage: II. Fast electron and ion characteristics versus neutron emission parameters and gun optimization perspectives. *Journal of Physics D-Applied Physics*, 2007. 40(12): 3592-3607.
16. Lee, S. and S.H. Saw. Neutron Scaling Laws from Numerical Experiments. *Journal of Fusion Energy*, 2008. 27(4): 292-295.
17. Lee, S., S.H. Saw, P. Lee, and R.S. Rawat. Numerical experiments on plasma focus neon soft x-ray scaling. *Plasma Physics and Controlled Fusion*, 2009. 51(10).
18. Lee, S., S.H. Saw, L. Soto, S.V. Springham, and S.P. Moo. Numerical experiments on plasma focus neutron yield versus pressure compared with laboratory experiments. *Plasma Physics and Controlled Fusion*, 2009. 51(7): 075006.
19. Akel, M. and S. Lee. Dependence of Plasma Focus Argon Soft X-Ray Yield on Storage Energy, Total and Pinch Currents. *Journal of Fusion Energy*, 2012. 31(2): 143-150.
20. Pimenov, V.N., E.V. Demina, S.A. Maslyaev, L.I. Ivanov, V.A. Gribkov, A.V. Dubrovsky, U. Ugaste, T. Laas, M. Scholz, R. Miklaszewski, B. Kolman, and A. Tartari. Damage and modification of materials produced by pulsed ion and plasma streams in Dense Plasma Focus device. *Nukleonika*, 2008. 53(3): 111-121.
21. Pimenov, V.N., Dubrovsky, A.V., Demina, E.V., Gribkov, V.A., Latyshev, S.V., Maslyaev, S.A., Sasinovskaya, I.P. and Scholz, M., (2013). Innovative powerful pulsed technique, based on a plasma accelerator, for simulation of radiation damage and testing of materials for nuclear systems.
22. Iwata, K., Haruki, T. and Sato, M., (2014). 2-D Particle-In-Cell Simulations of the Coalescence of Sixteen Current Filaments in Plasmas. *Plasma and Fusion Research*, 9(0), pp.3401072-3401072.

23. Gribkov, V.A., A. Srivastava, P.L.C. Keat, V. Kudryashov, and P. Lee. Operation of NX2 dense plasma focus device with argon filling as a possible radiation source for micro-machining. *Plasma Science, IEEE Transactions on*, 2002. 30(3): 1331-1338.
24. Lee, S., P. Lee, G.X. Zhang, Z.P. Feng, V.A. Gribkov, M. Liu, A. Serban, and T.K.S. Wong. High rep rate high performance plasma focus as a powerful radiation source. *Ieee Transactions on Plasma Science*, 1998. 26(4): 1119-1126.
25. Zhang, T., J. Lin, A. Patran, D. Wong, S.M. Hassan, S. Mahmood, T. White, T.L. Tan, S.V. Springham, S. Lee, P. Lee, and R.S. Rawat. Optimization of a plasma focus device as an electron beam source for thin film deposition. *Plasma Sources Science & Technology*, 2007. 16(2): 250-256.
26. Gribkov, V.A., S.V. Latyshev, R.A. Miklaszewski, M. Chernyshova, K. Drozdowicz, U. Wiacek, K. Tomaszewski, and B.D. Lemeshko. A dense plasma focus-based neutron source for a single-shot detection of illicit materials and explosives by a nanosecond neutron pulse. *Physica Scripta*, 2010. 81(3).
27. Benzi, V., F. Mezzetti, F. Rocchi, and M. Sumini. Feasibility analysis of a Plasma Focus neutron source for BNCT treatment of transplanted human liver. *Nuclear Instruments & Methods in Physics Research Section B-Beam Interactions with Materials and Atoms*, 2004. 213: 611-615.
28. Pouzo, J., M. Milanese, and R. Moroso. Portable Neutron Probe for Soil Humidity Measurements. *AIP Conference Proceedings*, 2003. 669(1): 277-280.
29. Koohestani, S., M. Habibi, and R. Amrollahi. Study of the effect of pyrex and quartz insulators on X-ray intensity in a 4 kJ plasma focus device. *European Physical Journal D*, 2013. 67(6).
30. Krauz, V.I. Progress in plasma focus research and applications. *Plasma Physics and Controlled Fusion*, 2006. 48(12B): B221-B229.
31. Shan, B. *Plasma dynamics and X-ray emission of the plasma focus*. Ph.D. Nanyang Technological University, Singapore; 2000.
32. Saw, S.H., P.C.K. Lee, R.S. Rawat, and S. Lee. Optimizing UNU/ICTP PFF Plasma Focus for Neon Soft X-ray Operation. *Ieee Transactions on Plasma Science*, 2009. 37(7): 1276-1282.
33. Lee, S. Plasma Focus Radiative Model: Review of the Lee Model Code. *Journal of Fusion Energy*, 2014. 33(4): 319-335.
34. Koh, J.M., R.S. Rawat, A. Patran, T. Zhang, D. Wong, S.V. Springham, T.L. Tan, S. Lee, and P. Lee. Optimization of the high pressure operation regime for enhanced neutron yield in a plasma focus device. *Plasma Sources Science & Technology*, 2005. 14(1): 12-18.
35. Schmidt, H., P. Kubes, M.J. Sadowski, and M. Scholz. Neutron emission characteristics of pinched dense magnetized plasmas. *Ieee Transactions on Plasma Science*, 2006. 34(5): 2363-2367.

36. Yousefi, H.R., S.R. Mohanty, Y. Nakada, H. Ito, and K. Masugata. Compression and neutron and ion beams emission mechanisms within a plasma focus device. *Physics of Plasmas*, 2006. 13(11).
37. Yousefi, H.R., Y. Nakada, H. Ito, and K. Masugata. Investigation of the neutron production mechanism in a 20 kJ plasma focus device. *Journal of Fusion Energy*, 2006. 25(3-4): 245-248.
38. Castillo, F., J.J.E. Herrera, and J. Rangel. Neutron yield and pressure evolution during a dense plasma focus device shot series. *Journal of Physics D-Applied Physics*, 2007. 40(19): 5902-5906.
39. Bruzzone, H., H. Acuna, and A. Clausse. Neutron correlations with electrical measurements in a plasma focus device. *Brazilian Journal of Physics*, 2008. 38(1): 117-122.
40. Roshan, M.V., R.S. Rawat, A. Talebitaher, P. Lee, and S.V. Springham. Neutron and high energy deuteron anisotropy investigations in plasma focus device. *Physics of Plasmas*, 2009. 16(5).
41. Borthakur, T.K. and A. Shyam. Analysis of axial neutron emission pulse from a plasma focus device. *Indian Journal of Pure & Applied Physics*, 2010. 48(2): 100-103.
42. Ablesimov, V.E., G.V. Karpov, and Z.S. Tsybikov. Correlation between the neutron yield from a plasma focus device and the jump in the discharge current. *Plasma Physics Reports*, 2012. 38(10): 820-823.
43. Bruzzone, H., M.O. Barbaglia, H.N. Acuna, M.M. Milanese, R.L. Moroso, and S. Guichon. On Probable Fusion Mechanisms in a Mather-Type Plasma Focus. *Ieee Transactions on Plasma Science*, 2013. 41(11): 3180-3183.
44. Castillo, F., M. Milanese, R. Morose, and J. Pouzo. Evidence of thermal and non-thermal mechanisms coexisting in dense plasma focus D-D nuclear reactions. *Journal of Physics D-Applied Physics*, 2000. 33(2): 141-147.
45. Abdou, A.E., M.I. Ismail, A.E. Mohamed, S. Lee, S.H. Saw, and R. Verma. Preliminary Results of Kansas State University Dense Plasma Focus. *Ieee Transactions on Plasma Science*, 2012. 40(10): 2741-2744.
46. Lee, S. Current and neutron scaling for megajoule plasma focus machines. *Plasma Physics and Controlled Fusion*, 2008. 50(10).
47. Nukulin, V.Y. and S.N. Polukhin. Saturation of the neutron yield from megajoule plasma focus facilities. *Plasma Physics Reports*, 2007. 33(4): 271-277.
48. Lee, S. Neutron yield saturation in plasma focus: A fundamental cause. *Applied Physics Letters*, 2009. 95(15).
49. Saw, S.H. and S. Lee. Scaling the plasma focus for fusion energy considerations. *International Journal of Energy Research*, 2011. 35(2): 81-88.
50. Talukdar, N., N.K. Neog, and T.K. Borthakur. Study on neutron emission from 2.2 kJ plasma focus device. *Physics of Plasmas (1994-present)*, 2014. 21(6): -.

51. Saw, S.H., D. Subedi, R. Khanal, R. Shrestha, S. Dugu, and S. Lee. Numerical Experiments on PF1000 Neutron Yield. *Journal of Fusion Energy*, 2014. 1-5.
52. Akel, M., Cikhardt, J., Kubes, P., Kunze, H. J., Lee, S., Paduch, M., & Saw, S. H. (2016). Experiments and simulations on the possibility of radiative contraction/collapse in the PF-1000 plasma focus. *Nukleonika*, 61(2), 145-148.
53. Cikhardtova, B., Kubes, P., Cikhardt, J., Paduch, M., Zielinska, E., Kravarik, J., Rezac, K. and Kortanek, J., 2016. Evolution of the small ball-like structures in the plasma focus discharge. *Nukleonika*, 61(2), pp.155-159.
54. Mitrofanov, K.N., Krauz, V.I., Grabovski, E.V., Myalton, V.V., Vinogradov, V.P., Paduch, M., Scholz, M. and Karpiński, L., 2015. Study of the interrelation between the electrotechnical parameters of the plasma focus discharge circuit and the plasma compression dynamics on the PF-3 and PF-1000 facilities. *Plasma Physics Reports*, 41(5), pp.379-398.
55. Sharif, M., S. Hussain, M. Zakaullah, and A. Waheed. Enhancement of X-ray emission in the side on direction in a Mather-type plasma focus. *European Physical Journal D*, 2006. 38(2): 337-341.
56. Eliseev, S.P., V.Y. Nikulin, and P.V. Silin. Correlation between Time-Resolved and Integral Measurements of the Soft X-Ray Emission in a Plasma Focus Operated in Argon. *Problems of Atomic Science and Technology*, 2008. (6): 216-218.
57. Eliseev, S.P., V.Y. Nikulin, and P.V. Silin. Measurement of Soft X-Ray Radiation using the PF-4 Plasma Focus Setup with Semiconductor X-Ray Detectors. *Bulletin of the Lebedev Physics Institute*, 2009. 36(1): 1-7.
58. Zavyalov, N. V., et al. "A source with a 10<sup>13</sup> DT neutron yield on the basis of a spherical plasma focus chamber." *Plasma Physics Reports* 39.3 (2013): 243-247.
59. Maslov, V.V., Rumyantsev, V.G., Basmanov, V.F. et al. *Instrum Exp Tech* (2014) 57: 131. doi:10.1134/S0020441214010254
60. Lee, S. and Saw, S.H., 2013. Plasma focus ion beam fluence and flux—for various gases. *Physics of Plasmas* (1994-present), 20(6), p.062702.
61. Shakya, A., Gautam, P. and Khanal, R., 2016. Comparison of Plasma Dynamics in Plasma Focus Devices PF1000 and PF400. *Journal of Nepal Physical Society*, 3(1), pp.55-59.
62. Afsharmanesh, M. and M. Habibi. Experimental study and analysis of multiple peaks in the SXR emitted from a 4 kJ plasma focus device. *European Physical Journal D*, 2013. 67(4).
63. Khan, M.Z., S.L. Yap, and C.S. Wong. Estimation of electron temperature and radiation emission of a low energy (2.2 kJ) plasma focus device. *Indian Journal of Physics*, 2014. 88(1): 97-102.
64. Akel, M., S. Al-Hawat, and S. Lee. Numerical Experiments on Soft X-ray Emission Optimization of Nitrogen Plasma in 3 kJ Plasma Focus SY-1 Using Modified Lee Model. *Journal of Fusion Energy*, 2009. 28(4): 355-363.

65. Lee, S., R.S. Rawat, P. Lee, and S.H. Saw. Soft x-ray yield from NX2 plasma focus. *Journal of Applied Physics*, 2009. 106(2).
66. Akel, M., S. Al-Hawat, S.H. Saw, and S. Lee. Numerical Experiments on Oxygen Soft X-Ray Emissions from Low Energy Plasma Focus Using Lee Model. *Journal of Fusion Energy*, 2010. 29(3): 223-231.
67. Akel, M., S. Al-Hawat, and S. Lee. Neon Soft X-Ray Yield Optimization from PF-SY1 Plasma Focus Device. *Journal of Fusion Energy*, 2011. 30(1): 39-47.
68. Al-Hawat, S., M. Akel, S. Lee, and S.H. Saw. Model Parameters Versus Gas Pressure in Two Different Plasma Focus Devices Operated in Argon and Neon. *Journal of Fusion Energy*, 2012. 31(1): 13-20.
69. Akel, M. and S. Lee. Practical Optimization of AECS PF-2 Plasma Focus Device for Argon Soft X-ray Operation. *Journal of Fusion Energy*, 2012. 31(2): 122-129.
70. Akel, M. Yield Optimization of Helium and Lyman Emissions in Low Energy Plasma Focus Operated with Argon. *Journal of Fusion Energy*, 2012. 31(5): 473-479.
71. Sharak, M.N., S. Goudarzi, A. Raeisdana, and M. Jafarabadi. Numerical Analysis of Amirkabir Plasma Focus (APF) Device for Neon and Argon Gases. *Journal of Fusion Energy*, 2013. 32(2): 258-262.
72. Lee, S. Plasma focus model yielding trajectory and structure. *Topical Conference on Radiation Plasmas*. World Scientific Publishing Co Pte.Ltd ,Singapore, 978-987.
73. Lee, S., A.S.I.C.f.T. Physics, Unesco, and A.A.A.f.P. Training. *Twelve Years of UNU/ICTP PFF: A Review*: Miramare. 1998.
74. Potter, D.E. Numerical Studies of the Plasma Focus. *Physics of Fluids (1958-1988)*, 1971. 14(9): 1911-1924.
75. Lee, P. and A. Serban. Dimensions and lifetime of the plasma focus pinch. *Plasma Science, IEEE Transactions on*, 1996. 24(3): 1101-1105.
76. Lee, S. Plasma focus experiments. *Proceedings of 1st Tropical College on Applied Physics: Laser and Plasma Technology*. 26th Dec 1983-14th Jan 1984 Kuala Lumpur: World Scientific Publishing Co., 1985. 38-62.
77. Lee, S. *Corona model*. 15 January 2014 [cited 2014; Available from: [www.plasmafocus.net/IPFS/modelpackage/Corona%20Calculations/C1coronaIntroduction.htm](http://www.plasmafocus.net/IPFS/modelpackage/Corona%20Calculations/C1coronaIntroduction.htm)].
78. Spitzer, L. *Physics of Fully Ionized Gases, in Interscience Tracts on Physics and Astronomy (2nd Revised Edition)*: Interscience Publication, New York. 1965.
79. Shearer, J.W. Contraction of Z pinches actuated by radiation losses. *Physics of Fluids (1958-1988)*, 1976. 19(9): 1426-1428.
80. Lee, S., S.H. Saw, and J. Ali. Numerical Experiments on Radiative Cooling and Collapse in Plasma Focus Operated in Krypton. *Journal of Fusion Energy*, 2013. 32(1): 42-49.

81. Huba, J.D. *NRL Plasma Formulary*. 2011 November 2013]; Available from: [http://wwwppd.nrl.navy.mil/nrlformulary/NRL\\_FORMULARY\\_07.pdf](http://wwwppd.nrl.navy.mil/nrlformulary/NRL_FORMULARY_07.pdf).
82. Lee, S. and S.H. Saw. Numerical Experiments Providing New Insights into Plasma Focus Fusion Devices. *Energies*, 2010. 3(4): 711-737.
83. Lee, S., S.H. Saw, A.E. Abdou, and H. Torreblanca. Characterizing Plasma Focus Devices—Role of the Static Inductance—Instability Phase Fitted by Anomalous Resistances. *Journal of Fusion Energy*, 2011. 30(4): 277-282.
84. Soto, L. New trends and future perspectives on plasma focus research. *Plasma Physics and Controlled Fusion*, 2005. 47: A361-A381.
85. Klir, D. and L. Soto. Drive Parameter of Neutron-Optimized Dense Plasma Foci. *Ieee Transactions on Plasma Science*, 2012. 40(12): 3273-3279.
86. Liu, M. *Soft X-rays from compact plasma focus*. Ph.D. Nanyang Technological University, Singapore; 2006.